

Advanced Eutectic Materials for Energy Storage: Ionic Liquids, Molten Salts, Deep Eutectic Solvents, Alloys, and Organic Cocrystals

Hu Hong, Xintao Ma, and Chunyi Zhi*

Eutectic materials are versatile for energy storage and conversion due to their tunable composition, depressed melting temperatures, and enhanced ionic conductivity. This review surveys recent developments in eutectic materials, including ionic liquids, molten salts, deep eutectic solvents, alloy materials, and organic cocrystals. The fundamental parameters that dictate eutectic

performance, including phase diagram control, component ratios, and thermal stability are analyzed, and its advantages in various aspects of application are summarized. This review concludes with some outlooks for developing energy storage using eutectic materials.

1. Introduction

Under the carbon-neutral strategy, building a new power system dominated by renewable energy has become a global consensus. The large-scale integration of intermittent clean sources such as wind and solar power poses severe challenges to grid stability and urgently requires the development of efficient and reliable energy storage technologies for spatiotemporal balancing of supply and demand. Electrochemical energy storage has emerged as a key enabling technology because of its high energy conversion efficiency, fast response, and flexible modular deployment.^[1] A typical electrochemical storage device such as lithium-ion, sodium-ion, or potassium-ion battery consists of four core components: a positive electrode, a negative electrode, a separator, and an electrolyte.^[2] Performance optimization demands coordinated advances in electrode material innovation, electrolyte-interface engineering, and system integration.

In recent years, eutectic materials have shown broad potential in the energy storage field owing to their unique synergistic interactions and tunable physicochemical properties.^[3] As homogeneous multicomponent systems held together by noncovalent forces, eutectic materials overcome the performance limitations of single-component materials.^[4] Deep eutectic solvents (DESs) reconstruct hydrogen-bond networks in liquid systems to achieve high ionic conductivity and wide electrochemical stability windows.^[5] In solid systems, eutectic alloys attain exceptional mechanical strength and cycling stability through controlled intermixing of constituent elements.^[6] Today, eutectic materials have been incorporated into multiple key battery components, including ionic-liquid electrolytes, molten salt heat-transfer

media, and organic eutectic electrode materials. However, most studies focus on the performance characterization of specific systems and lack a systematic summary of structure–property relationships and component synergy mechanisms. This gap hinders the targeted design of high-performance eutectic materials.

This review summarizes the applications of eutectic materials in the field of energy storage, including ionic liquids, molten salts, DESs, alloy materials, and organic cocrystals. Then, the challenges and future development directions of eutectic materials in energy storage are discussed to provide a valuable reference for researchers to develop high-performance eutectic materials.

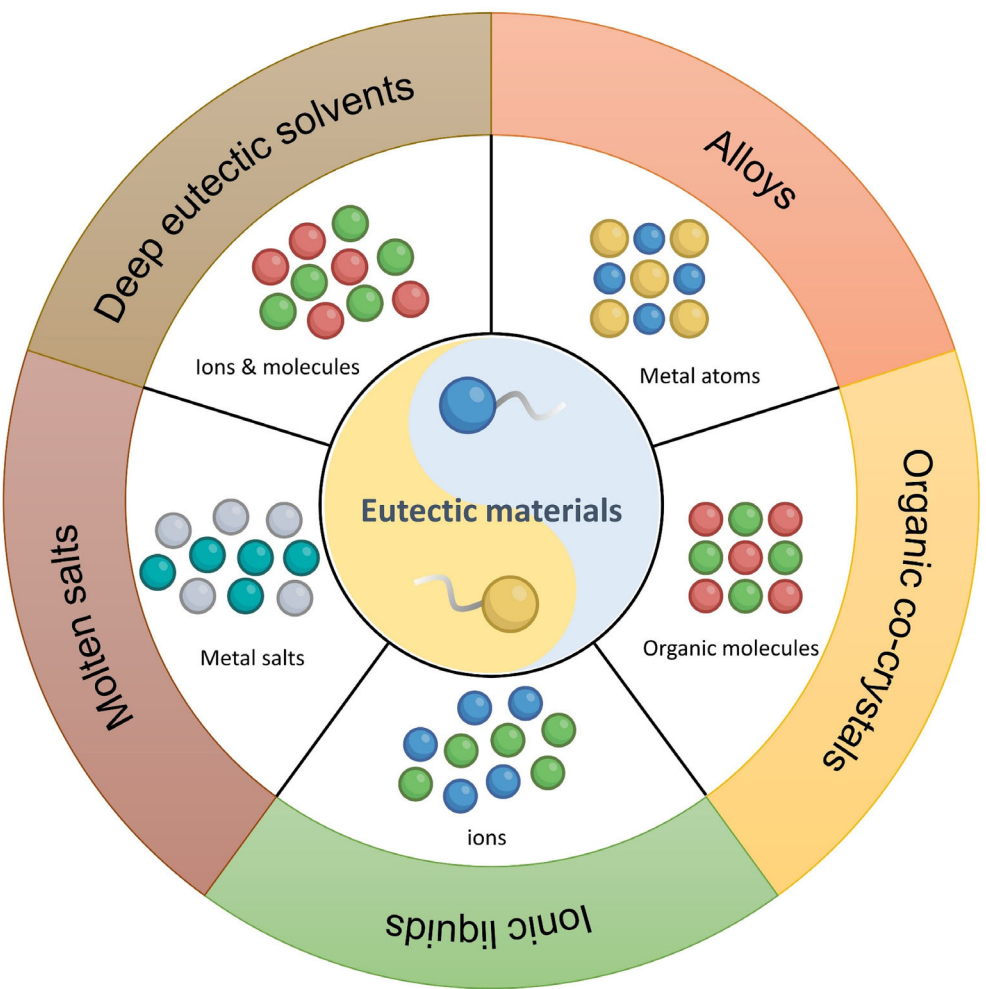
2. The Formation of Eutectics

The term “eutectic” originated in metallurgy and has gradually gained attention in recent decades, playing an important role in various fields such as electronic devices, semiconductor engineering, chemical engineering, and separation technology.^[7] However, many researchers still consider eutectics to be of interest primarily to physical chemistry experts, with limited appeal to the average chemistry reader. Although there are already quite a few reviews on eutectics, most provide a deep overview of a specific class of eutectic systems.

The properties and application ranges of eutectic systems vary significantly. For instance, while there is considerable research on eutectic metals in electronics, reviews and research on their dissolution and separation aspects are relatively scarce. Additionally, although there is a wealth of literature on the application of eutectic salts in energy storage, their role in environmental science is less explored. In fact, DESs have shown tremendous potential for application in environmental science and separation science. In some fields, including battery technology, these eutectics have cross-applications (**Scheme 1**).

A notable example of eutectic application is the Hall–Héroult process. By forming a eutectic system with Na_3AlF_6 (melting point

H. Hong, X. Ma, C. Zhi
Department of Materials Science and Engineering
City University of Hong Kong
83 Tat Chee Avenue, Kowloon, Hong Kong 999077, China
E-mail: cy.zhi@cityu.edu.hk



Scheme 1. Schematic of eutectic materials for energy storage.

1010 °C), aluminum electrolysis can occur at around 960 °C. Furthermore, the reduction of the melting point has facilitated advancements in welding technology. The original meaning of

"eutectic" is easily melted, which we interpret as "a lowering of the melting point upon mixing."^[8] Generally speaking, most substances are composed of atoms, ions, or molecules, and



Hu Hong received his B.E. degree from Central South University in 2017 and his M.S. degree from South China University of Technology in 2020. He obtained his Ph.D. degree in 2025 under the supervision of Professor Chunyi Zhi. His research interests focus on the development of eutectic materials for energy storage and conversion.



Chunyi Zhi obtained his Ph.D. in physics from the Institute of Physics, Chinese Academy of Sciences. He subsequently worked as a post-doctoral researcher at the National Institute for Materials Science (NIMS) in Japan, followed by a research fellow at the International Center for Young Scientists at NIMS and a senior researcher at NIMS. Currently, he is a Chair Professor in the Department of Materials Science and Engineering at City University of Hong Kong. His research interests include aqueous zinc-ion batteries, flow batteries, solid-state batteries, and catalysts for sustainable development.



Xiantao Ma received his M.S. degree from Xiamen University in 2023, where his research focused on electrocatalytic CO₂ reduction for high-value chemical production. Since 2024, he has been pursuing a Ph.D. degree at City University of Hong Kong under the supervision of Professor Chunyi Zhi. His current research interests encompass the development of aqueous zinc-based batteries, flow batteries, electrocatalytic energy conversion technologies, and the design and synthesis of advanced catalysts.

the types of binary systems that can form are illustrated in **Figure 1**. The essence of metals is atomic; therefore, eutectic metals can be viewed as an eutectic mixture of atoms. Eutectic salts consist of systems made up of anions and cations, which can also include ions and molecules.

In contrast to the more specific eutectic systems mentioned above, we can extend the concept of eutectics to a broader definition. This broader eutectic should encompass all mixed systems where the interactions between the components are stronger than those within each individual component, manifesting macroscopically as a lowered melting point (**Figure 2**). The degree of mixing among these systems generally increases, indicating that the eutectic process is an entropy-increasing process.

These systems often exhibit characteristics different from their individual components. A common example is electrolytes, which are formed by dissolving salts in a solvent. In this process, metal salts become solvated by solvent molecules, resulting in enhanced ionic conductivity in the electrolyte.^[9] To achieve good conductivity, it is typically believed that this must occur in the liquid state; however, solid and liquid states are merely different physical states dependent on their melting points. Substances with melting points below room temperature are considered

room-temperature liquids. For instance, ionic molten salts are composed of different metal salts mixed together, exhibiting good ionic conductivity at high temperatures, and are often used as electrolytes.

Beyond their use in liquid form, eutectic systems can also serve as precursors for manufacturing electrode materials. By mixing two pure components, new materials can be obtained. This entirely relies on the stronger interactions between the different components compared to those between their individual molecules. Understanding electrochemical energy storage systems from this perspective can provide new insights and discoveries, although this direction is rarely explored. The formation of eutectics involves a specific mechanism that dictates how two or more components interact during cooling or solidification in a mixture.^[10] At the heart of eutectic formation is the concept of phase equilibrium, where the system reaches a state of stability at a particular composition and temperature. As a mixture of two or more components is cooled from a liquid state, the eutectic point is reached at a specific composition, known as the eutectic composition, where the liquid phase solidifies into two distinct solid phases simultaneously.

A liquid mixture undergoes a series of changes when it approaches the eutectic temperature. Initially, as the temperature decreases, the liquid begins to lose energy, facilitating solid phase formation. However, unlike in noneutectic systems, where one phase might solidify before another, both solid phases nucleate and grow concurrently in a eutectic system. This simultaneous solidification is driven by the specific interactions between the molecules of the components, particularly hydrogen bonding, van der Waals forces, and coordination chemistry. The nucleation process is critical in eutectic formation (**Figure 3**). Nucleation can occur either homogeneously, where clusters of molecules spontaneously form within the liquid, or heterogeneously, where nucleation occurs on existing surfaces or impurities. The presence of certain impurities or pre-existing solid phases can promote heterogeneous nucleation, influencing the formation and growth rate of the solid phases. As the liquid reaches the eutectic temperature, it becomes supersaturated with respect to both solid phases, leading to the rapid growth of these solids.^[11]

The resulting microstructure typically exhibits a fine, lamellar or fibrous arrangement of the two solid phases during solidification. This unique microstructure arises from the competition between the growth rates of the two phases, which are influenced by factors such as temperature, composition, and the specific interactions between the components.^[12] The interdiffusion of atoms or molecules at the solid–liquid interface plays a significant role in maintaining the equilibrium of phases during this process.

As the eutectic solidification progresses, the final microstructure is characterized by a homogeneous distribution of the two solid phases, which can enhance the material's overall properties, such as strength, hardness, and wear resistance. The specific arrangement and distribution of the solid phases depend on the eutectic mixture's cooling rate and compositional factors. Rapid cooling can lead to finer microstructures, while slower cooling allows for more pronounced phase separation and coarsening

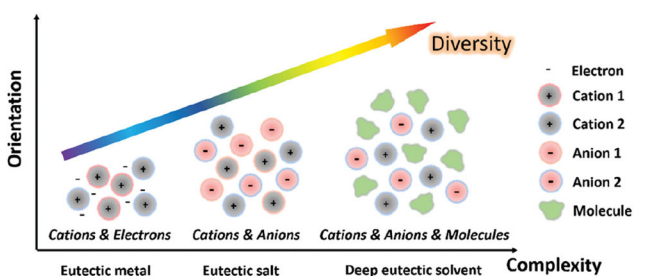


Figure 1. Comparison of three different eutectics. Reproduced with permission.^[8] Copyright 2021, Royal Society of Chemistry.

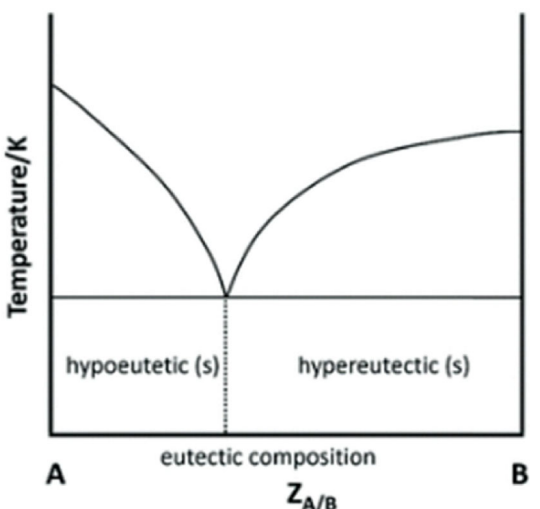


Figure 2. Hypoeutectic and hypereutectic regions are on both sides of eutectic composition. Reproduced with permission.^[8] Copyright 2021, Royal Society of Chemistry.

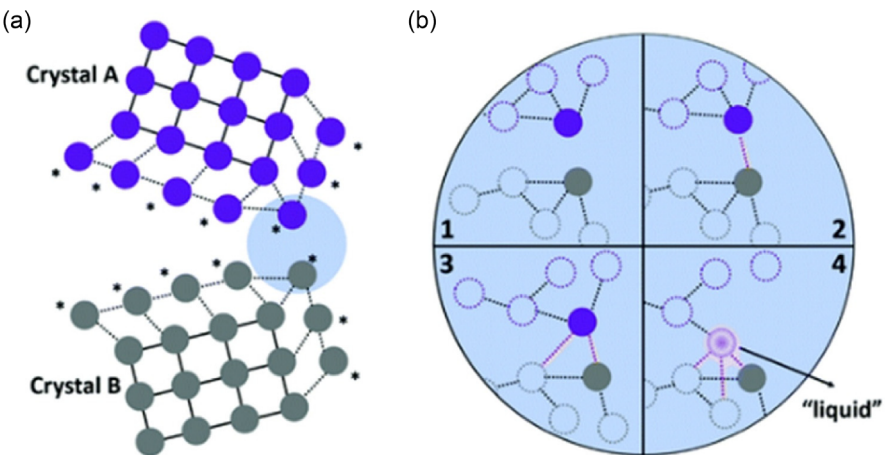


Figure 3. a) Schematic of contact between two crystals. The crystal atoms (labeled by *) on the surface have a low coordination number and can be regarded as activated atoms. b) A diagram illustrates how a “liquid” atom is generated. Reproduced with permission.^[8] Copyright 2021, Royal Society of Chemistry.

of the microstructure. In summary, the formation of eutectics involves a complex interplay of phase equilibrium, nucleation, and solidification mechanisms, resulting in the simultaneous growth of two distinct solid phases from a liquid mixture. Understanding these properties and applying them to the field of electrochemical energy storage will provide unexpected perspectives.

3. Liquid Eutectic Materials

3.1. Ionic Liquids

Ionic liquids date back to early studies of molten salts in the 19th century, but the label “ionic liquid” appeared only in the late 20th century for salts that remain liquid at room temperature. In the 1990s, researchers first synthesized room-temperature versions based on imidazolium and pyridinium cations, with 1-butyl-3-methylimidazolium hexafluorophosphate (BMIM PF₆) prepared in 1992 becoming especially important because of its negligible vapor pressure and excellent thermal stability. That breakthrough led to a systematic exploration of other cation–anion pairs to tune properties. Recognizing their environmental advantages over volatile organic solvents, scientists investigated ionic liquids as greener media for catalysis, electrochemistry, and separation processes.^[13] By the early 2000s, the field had grown rapidly, establishing ionic liquids as versatile, sustainable alternatives in many areas of chemistry.

Throughout the years, the academic and industrial interest in ionic liquids has grown exponentially. They have been the subject of numerous conferences, workshops, and dedicated research programs. The increasing awareness of the need for sustainable and environmentally friendly chemical processes has further fueled the exploration of ionic liquids as viable alternatives to traditional solvents.^[14] Next, we will introduce the applications of ionic liquids in the field of electrochemistry.

Aluminum-ion batteries primarily use ionic liquids as mainstream electrolytes in these different ion-conducting batteries. In 2015, Dai et al. reported an aluminum metal battery using AlCl₃/1-ethyl-3-methylimidazolium chloride (AlCl₃/[EMIm]Cl) IL as the electrolyte,^[15] aluminum metal as the anode, and graphite as the cathode (Figure 4). The voltage reached up to 2.2 V, although the capacity was not high, only 66 mA h g⁻¹. This was the first rechargeable aluminum-ion battery. This battery system exhibits excellent safety thanks to the nonvolatile and nonflammable nature of ionic liquids.

Zinc-ion batteries (ZIBs) are widely studied as next-generation energy storage systems due to their high safety and low cost.^[16] However, key issues such as irregular dendrite growth and complex side reactions severely hinder the further industrialization of ZIBs^[17]. Chen et al.^[18] proposed a strategy for preparing a semi-fixed ionic liquid interfacial layer to protect the Zn anode over a wide temperature range of –35 to 60 °C. The fixed SiO₂@cation (Zn@SIP) can form a highly conjugated framework that regulates the Zn²⁺ concentration gradient and the self-polarization electric field, ensuring uniform nucleation and planar deposition. The free anions in the ionic liquids can weaken the hydrogen bonding of water, facilitating the rapid desolvation of Zn²⁺ and simultaneously accelerating ion transport kinetics (Figure 4).

In addition to the ionic channel layer that protects the anode, Chen Chaoji et al.^[19] reported a water-immiscible ionic liquid diluent, 1-ethyl-3-methylimidazolium bis(fluorosulfonyl)imide (EmimFSI), which can significantly suppress the water activity in aqueous electrolytes by acting as a “water bag.” This diluent encapsulates high-activity H₂O-based Zn²⁺ solvates and protects them from parasitic reactions. During the Zn deposition process, the cation Emim⁺ and the anion FSI⁻ serve to alleviate the tip effect and regulate the solid electrolyte interphase (SEI), thereby facilitating the formation of a smooth Zn deposition layer. This deposited layer is protected by an SEI rich in inorganic materials, which exhibits high uniformity and stability (Figure 5).

The evolution of ionic liquids from obscure chemical curiosities to essential materials in modern science illustrates

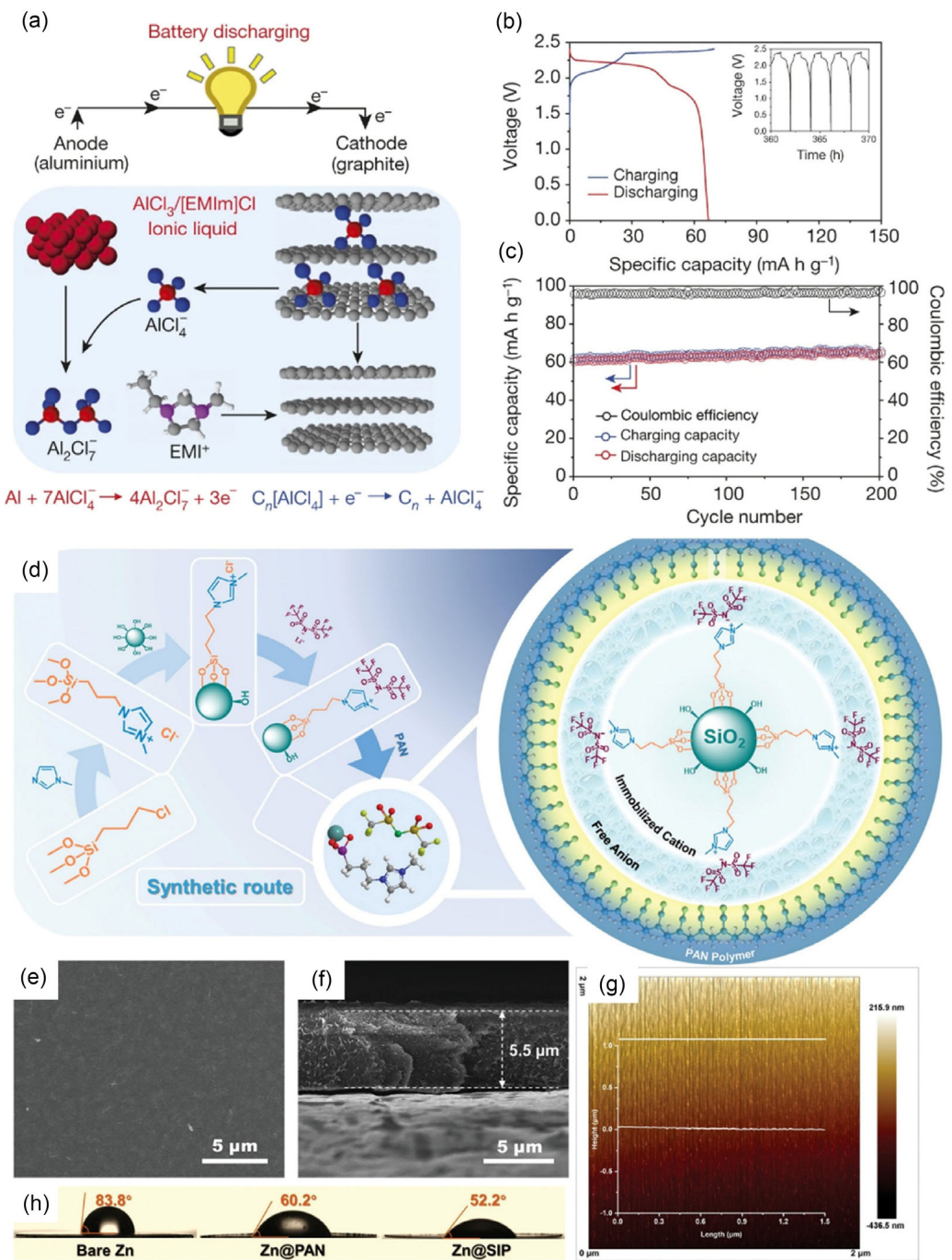


Figure 4. a) Schematic drawing of the Al/graphite cell during discharge, using the optimal composition of the $\text{AlCl}_3/\text{[EMIm]Cl}$ ionic liquid electrolyte. b) Galvanostatic charge and discharge curves of an Al/pyrolytic graphite Swagelok cell at a current density of 66 mA g^{-1} . c) Corresponding cycling performance of an Al/pyrolytic graphite Swagelok cell. Reproduced with permission.^[15] Copyright 2015, Springer Nature. d) Schematic illustration for the synthetic route of the SIP polymer. e,f) Top-view and cross-sectional scanning electron microscopy (SEM) images of the Zn@SIP anode. g) Atomic force microscopy (AFM) image of the Zn@SIP surface. h) Digital photos of the contact angle between various zinc anodes and electrolytes. Reproduced with permission.^[18] Copyright 2022, Wiley-VCH.

the dynamic nature of research and the continuous quest for more efficient and sustainable methods in chemistry and engineering. As the field advances, ionic liquids are expected to play an increasingly significant role in addressing global challenges related to energy, environment, and materials science.

3.2. Molten Salts

Molten salts have garnered significant attention in the field of electrochemistry due to their unique properties, making them suitable for various applications. One of their most notable uses is electrolytes in high-temperature batteries, such as sodium-sulfur

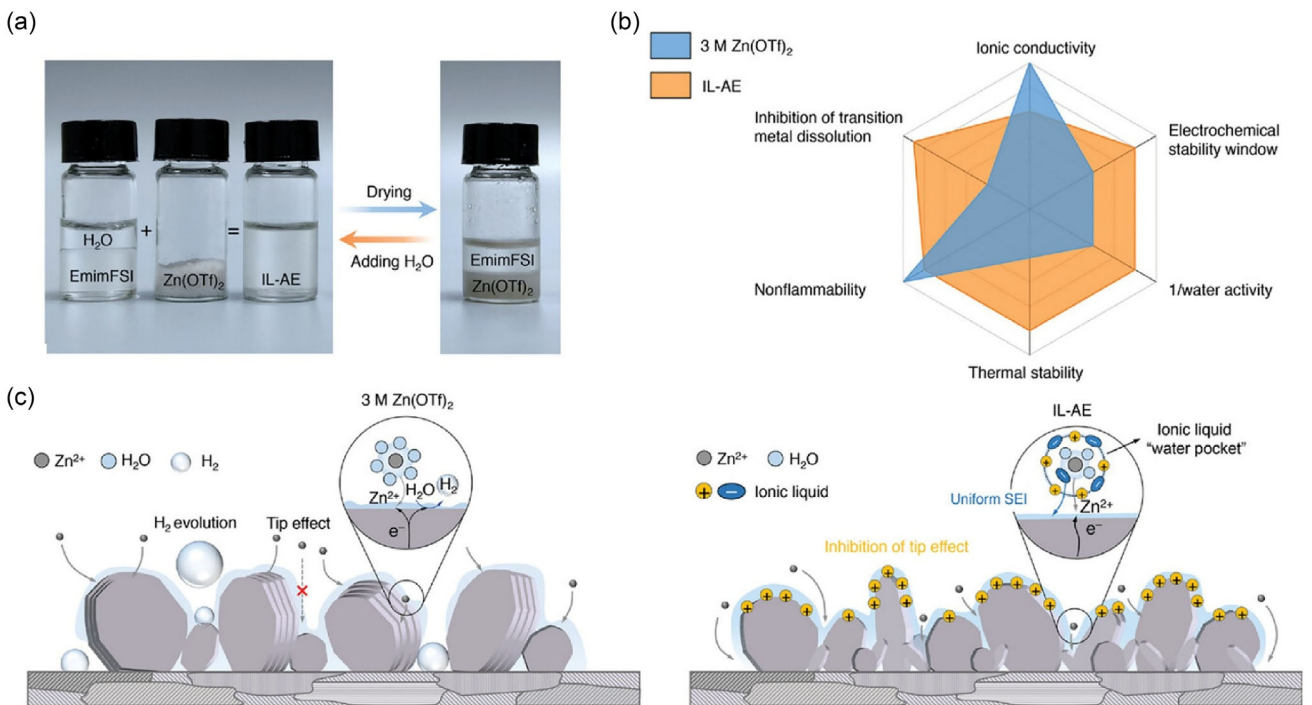


Figure 5. a) Digital photos showing the immiscible binary H₂O-EmimFSI system becoming a homogeneous solution with the addition of Zn(OTf)₂. b) Radar plots comparing the performance, in which the results are normalized by the maximum value of each characteristic. c) Schematic illustrating the solvation/desolvation and Zn deposition chemistry of the two electrolytes. Reproduced with permission.^[19] Copyright 2023, Wiley-VCH.

and molten salt batteries. These systems benefit from the high ionic conductivity of molten salts at elevated temperatures, which enhances ion transport efficiency and improves energy storage capabilities. Operating at high temperatures also helps minimize electrolyte degradation, contributing to longer battery life. In addition to batteries, molten salts are extensively used in electrochemical cells and reactors, serving as media that facilitate ionic transport. In fuel cells, for instance, they provide a stable environment for electrochemical reactions, enabling more efficient conversion of chemical energy into electrical energy. Their stability under varying temperature and pressure conditions makes them ideal for applications in both stationary and portable power sources. Molten salts also play a crucial role in the electrorefining and electrowinning of metals. Acting as solvents that dissolve various metal salts, they facilitate extracting and purifying valuable metals from ores and industrial waste. This process enhances metal recovery efficiency, making molten salts attractive for sustainable resource management, particularly in recycling electronic waste and other secondary materials. Moreover, molten salts are utilized in various sensors and electrochemical devices. Their stable ionic environment allows for accurate measurements and improved performance in sensing applications, such as detecting gases or monitoring environmental conditions.

Molten salts form deep eutectic mixtures when the introduction of a hydrogen-bond donor (HBD) or other coordinating partner such as urea, glycerol, or ethylene glycol into a crystalline ionic lattice both disrupts the original ion–ion interactions and generates a highly disordered hydrogen-bond network.

As a result, the free energy of melting becomes negative at temperatures far below those of the individual components. Concurrently, partial charge delocalization through hydrogen bonding or coordination to the anion reduces cation–anion attraction and extends the liquid-phase region. To understand the functional advantages of these eutectic liquids, one must consider how the depressed melting point and intricate hydrogen-bond/ionic network enhance ionic mobility, modify solvation shells of reactive species to shift redox potentials, promote substrate diffusion in catalysis and extraction, and stabilize interfaces in electrochemical cells—all mechanisms that underpin the superior performance of DES in catalytic, separation, and energy storage applications.

Pan et al.^[20] developed a bidirectional, fast-charging aluminum–sulfur group element battery using a molten salt electrolyte composed of NaCl–KCl–AlCl₃ (Figure 6a–f). These aluminum chloride melts contain a high concentration of AlCl₃ and include chain-like Al_nCl_{3n+1} species, such as Al₂Cl₇[−], Al₃Cl₁₀[−], and Al₄Cl₁₃[−], which facilitate simple Al³⁺ desolvation kinetics through Al–Cl–Al bonds, leading to a high Faradaic exchange current and establishing the foundation for high-rate charging of the battery. This chemical reaction differs from other aluminum batteries in that it utilizes sulfur group element electrodes as the cathode rather than various low-capacity compound formulations, and it opts for molten salt electrolytes instead of room-temperature ionic liquids that induce high polarization. This molten salt electrolyte system can support rapid charging and discharging rates without forming dendrites. These unique features are gradually being uncovered.

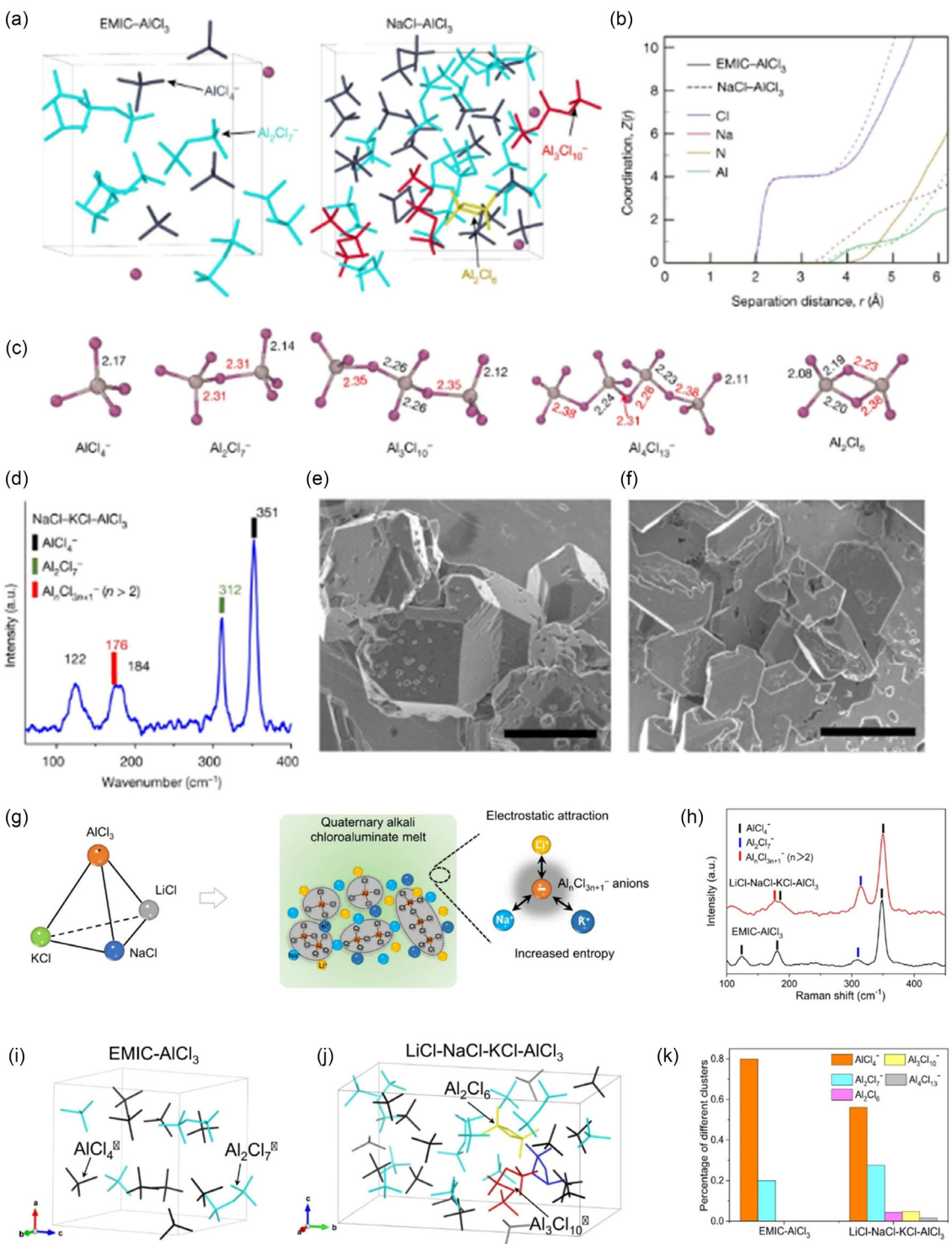


Figure 6. a) Typical snapshots from the Ab initio molecular dynamics (AIMD) trajectories showing the different chloroaluminate solvation clusters for the two electrolytes; Cl⁻, AlCl₄⁻, Al₂Cl₆, Al₂Cl₇⁻, and Al₃Cl₁₀⁻ clusters are shown in purple, dark blue, gold, cyan, and red, respectively. b) The atomic coordination around Al³⁺, Z(r), as a function of bonding distance, r, by integrating the radial distribution functions obtained from AIMD simulations. c) The representative configuration of the clusters taken from the calculated equilibrium states; the Al and Cl atoms are shown in gray and purple, respectively. d) The Raman spectrum of the NaCl-KCl-AlCl₃ electrolyte measured at 180 °C. e,f) The SEM images of Al plated on a Ta substrate in the molten NaCl-KCl-AlCl₃ electrolytes at 180 °C. Reproduced with permission.^[20] Copyright 2022, Springer Nature. g) Tetrahedral diagram of the four components for inorganic molten salt electrolyte, showing the basis for the phase diagram for the electrolyte formulations. h) Raman spectra of the quaternary alkali chlороaluminate melt (LiCl-NaCl-KCl-AlCl₃) and ionic liquid (EMIC-AlCl₃) electrolytes. i,j) Typical snapshots from the AIMD trajectories in equilibrium showing the different solvation clusters for the organic ionic liquid and quaternary alkali melt electrolytes. k) Percentage of different Al-Cl clusters in the quaternary alkali melt and ionic liquid electrolytes, as quantified from AIMD trajectories.

They subsequently reported a fast-charging aluminum–sulfur battery that operates at a sub-boiling temperature of 85 °C,^[21] utilizing a tailored quaternary molten salt electrolyte (Figure 6g–k). The quaternary alkali metal aluminum chloride melts feature abundant electrochemically active higher order Al–Cl clusters and a lower melting point, facilitating rapid Al³⁺ desolvation. Nitrogen-functionalized porous carbon further mediates the sulfur reaction, enabling the battery to achieve fast charging capabilities and excellent cycling stability, with a capacity retention of 85.4% after 1400 cycles at a 1 C charging rate. This molten salt exhibits excellent electrochemical performance, is easy to prepare, and is cost-effective.

Single-crystal layered cathodes are often ideal materials for advanced lithium-ion batteries. However, challenges remain in producing single-crystal cathodes with high phase purity, good electrochemical performance, and scalability due to limitations in the achievable temperature range that cannot prevent lithium evaporation, lattice defects, and particle agglomeration. Li et al.^[22] invented a novel mechanochemical activation process that provides a universal solution to the challenge of synthesizing lithium/manganese-rich or nickel-rich coarse single-crystal cathodes, differing from the equipment- and energy-intensive methods that are difficult to scale (Figure 7). This approach is based on interfacial reaction wetting, mediated by moderately mechanical stirring of *in situ* molten transient eutectic salts, forming a colloidal suspension of nano-oxides dispersed in liquefied lithium salts. This effectively depolymerizes the polycrystalline precursors, refills the crystals, and ensures uniform distribution of lithium salts, making it easier for the particles to subsequently coarsen into a single-crystal form, thereby improving electrochemical performance. This method of preparing cathode materials assisted

by molten salts cleverly utilizes the properties of molten salts, demonstrating their promising application potential.

Overall, the unique properties of molten salts, including low volatility, high thermal stability, and tunable ionic conductivity, make them valuable for advancing electrochemical technologies. Ongoing research aims to optimize molten salt compositions to enhance performance in specific applications, further establishing their role in the future of electrochemistry. As innovations continue to emerge, molten salts are poised to play a crucial role in addressing challenges in energy storage, metal recovery, and sustainable practices across various industries.

3.3. DESs

DESs have emerged as a significant class of solvents in recent years, characterized by their unique properties and versatility in various applications.^[7,23] These solvents are formed by mixing a Lewis acid and a Lewis base, resulting in a eutectic mixture that exhibits a melting point significantly lower than that of the individual components. DESs offer a range of advantages, including low toxicity, biodegradability, and tunable properties, making them attractive alternatives to traditional organic solvents. The concept of DESs was first introduced in the early 2000s, primarily to develop greener solvents that could replace volatile organic compounds (VOCs) in chemical processes. The ability to design DESs with specific properties by varying the components opened up new avenues for research and application in fields such as extraction, catalysis, electrochemistry, and material science. The history of DESs can be traced back to the study of eutectic mixtures, with roots in metallurgy and crystallization. The term “eutectic” refers to a specific composition of two or more

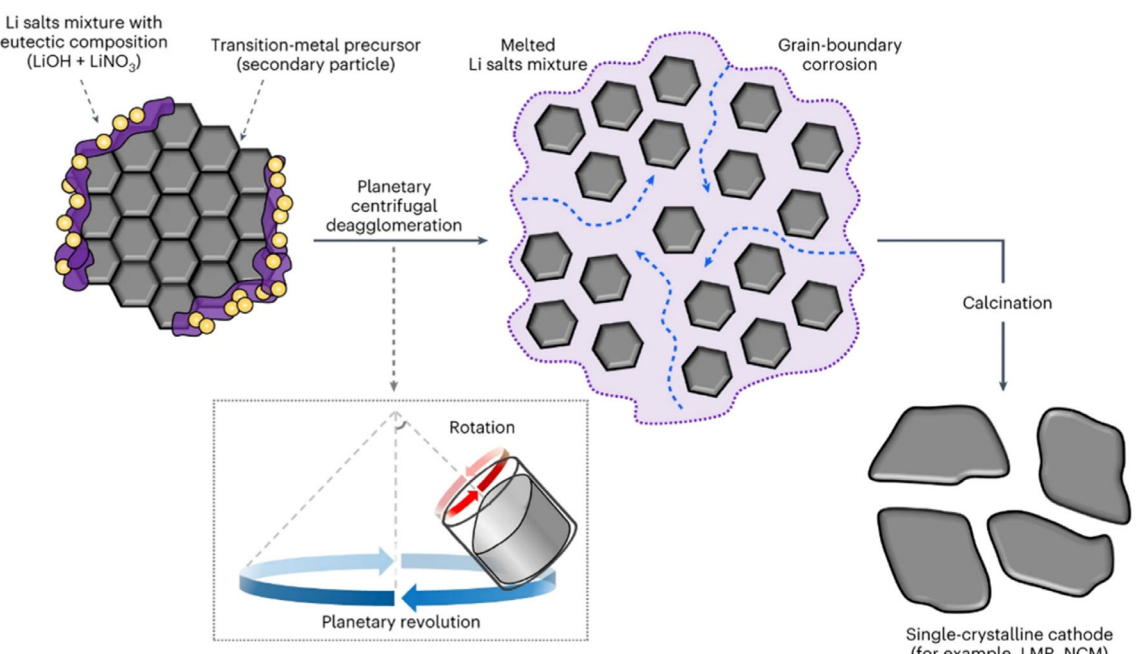


Figure 7. Schematic diagram of synthesizing manganese/nickel-rich lithium battery positive electrode materials using the eutectic principle. Reproduced with permission from.^[22] Copyright 2023, Springer Nature.

substances that melt at a lower temperature than any of the individual components. Early research focused on understanding the phase behavior of these mixtures and their applications in various industries.

The modern development of DESs began with the work of researchers aiming to create environmentally friendly solvents. In 2003, Abbott and colleagues reported the first DES, which explored the use of choline chloride and urea as a solvent system. This mixture demonstrated significant advantages over traditional solvents, prompting further investigation into DESs formed from various combinations of HBDs and acceptors. DESs are typically composed of a HBD and a hydrogen bond acceptor (HBA). The selection of HBDs and HBAs can significantly influence the properties of the resulting DES, such as viscosity, density, and thermal stability.^[24] Common HBDs include urea, glycerol, and various organic acids, while HBAs often include quaternary ammonium salts like choline chloride. The properties of DESs can be tailored for specific applications by adjusting the ratios of the components. For example, increasing the proportion of the HBD can lead to lower viscosity and improved solvation properties, while altering the HBA can impact the thermal stability and conductivity of the solvent. This tunability is one of the key advantages of DESs, allowing researchers to design solvents optimized for particular tasks.

DESs offer several advantages over traditional organic solvents. One of the most significant benefits is their low toxicity,^[23,25] which makes them safer for both human health and the environment. Many DESs are composed of natural or biodegradable components, contributing to their appeal as greener alternatives to conventional solvents. Additionally, DESs exhibit low vapor pressure, reducing the risk of air pollution and occupational exposure associated with VOCs. This property makes them suitable for use in closed systems and processes where solvent evaporation is a concern. The ability to dissolve a wide range of substances is another advantage of DESs. DESs can effectively solvate both polar and nonpolar compounds, making them versatile for various chemical reactions and extraction processes. Their unique solvation capabilities enable the dissolution of biomolecules, metals, and salts, which can be particularly useful in fields such as biochemistry and materials science.

DESs have found applications in a wide range of fields, driven by their unique properties and advantages. They are increasingly used in extraction processes for natural products, metals, and biomolecules. Their ability to dissolve a wide range of compounds makes them effective for extracting valuable components from complex mixtures, such as plant extracts or mineral ores. In catalytic processes, DESs can serve as reaction media that enhance the efficiency of catalysts. They can stabilize reactive intermediates and facilitate reaction pathways, leading to improved yields and selectivity. Additionally, DESs are being explored as electrolytes in batteries and supercapacitors due to their high ionic conductivity and electrochemical stability.^[3a] Their unique properties allow for better ion transport and energy storage capabilities compared to traditional electrolyte solutions. Moreover, DESs are utilized in various sensors and electrochemical devices. Their stable ionic environment allows for accurate measurements

and improved performance in sensing applications, such as detecting gases or monitoring environmental conditions. Researchers are also exploring their integration into energy conversion processes, including thermochemical cycles, where they can enhance the efficiency of reactions for hydrogen production and carbon capture. The move toward using DESs is driven in part by the need for more sustainable and environmentally friendly chemical processes. DESs, often composed of biodegradable and nontoxic components, present a lower environmental impact compared to traditional solvents. Their low vapor pressure and reduced volatility contribute to a safer working environment and lower emissions of harmful solvents into the atmosphere. Research continues to explore the life cycle of DESs, including their production, use, and disposal, to ensure that they are genuinely sustainable alternatives. The development of methods for recycling and reusing DESs is also a focus, as this can further minimize waste and enhance the sustainability of chemical processes.

DESs are most commonly used to dissolve various substances. For example, Pulickel M. Ajayan et al.^[26] demonstrated a method for recycling Lithium-ion batteries (LIBs) using DESs to extract valuable metals from various chemicals, including lithium cobalt (III) oxide and nickel manganese cobalt lithium (Figure 8). For the extraction of metals from lithium cobalt (III) oxide, both cobalt and lithium leaching efficiencies reached $\geq 90\%$. It was also found that other battery components, such as aluminum foil and polyvinylidene fluoride binders, could be recovered separately. DESs offer a green alternative to traditional LIB recycling methods, allowing for the recovery of strategically important metals, which is crucial for meeting the exponentially growing demand for LIB production. This recycling method effectively utilizes DESs' green and customizable properties, showcasing their strong application potential.

Another popular application of DES is as electrolytes. For example, Cui et al.^[27] proposed a novel aqueous eutectic electrolyte that alleviates these issues by coupling hydrated Zn salts ($Zn(ClO_4)_2 \cdot 6H_2O$) with a neutral ligand (dinitrile). The unique hydrated Zn^{2+} solvates feature a dinitrile-assisted solvation shell, enabling unusual Zn/Zn^{2+} reversibility with a Coulombic efficiency of up to 98.4% while ensuring smooth Zn deposition. Additionally, all water molecules contribute to forming a eutectic network, thereby delaying oxidation and suppressing solvation capability (Figure 9a–g). Wang et al.^[28] also reported a 4.5 m lithium bis(trifluoromethanesulfonyl)imide (LiTFSI)-KOH-CO(NH₂)₂-H₂O non-flammable ternary eutectic electrolyte (Figure 9h–m), which expands the electrochemical stability window to >3.3 V by forming a robust SEI. This ternary eutectic electrolyte enables Li_{1.5}Mn₂O₄||Li_xTi₅O₁₂ pouch cells to achieve a high average Coulombic efficiency of 99.96% and a capacity retention of 92% after 470 cycles under conditions of an areal capacity of 2.5 mA h cm⁻², a cathode/anode capacity ratio of 1.14, and a thin electrolyte (3 g Ah⁻¹). Delrue De Sloovere et al. reported that a nonflammable DESs, formed by dissolving NaTFSI in *N*-methyl acetamide (NMA), can enhance the stability of sodium-ion batteries. Increasing NaTFSI concentration strengthens ionic interactions, lowers the HOMO level of NMA, and raises the anodic stability to ≈ 4.65 V versus Na⁺/Na. The formation of robust

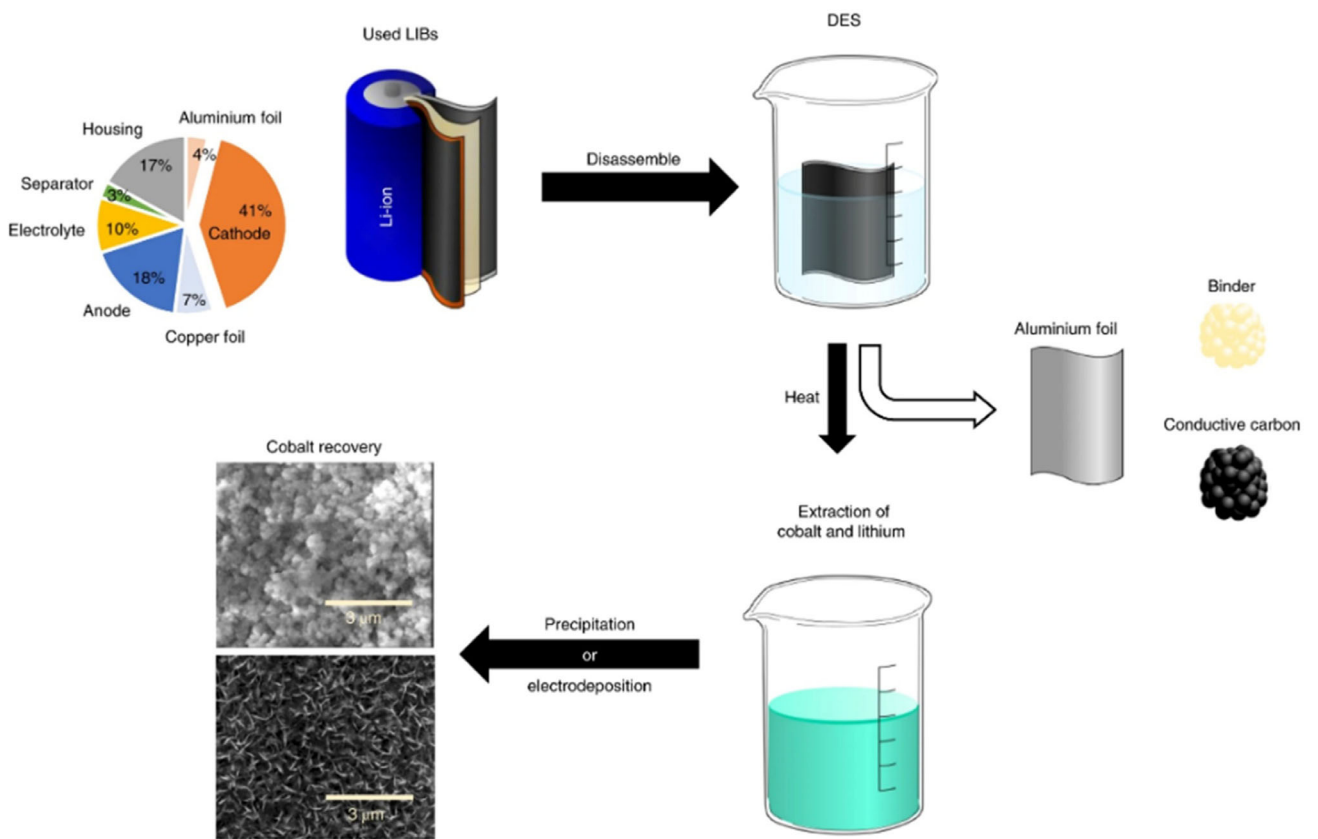


Figure 8. Flow chart of using DES to recover valuable materials from lithium-ion batteries. Reproduced with permission from.^[26] Copyright 2019, Springer Nature.

interfacial films improves cycling performance, highlighting the potential of DESs as safe and effective electrolyte alternatives.^[29]

Future research directions include exploring new combinations of HBDs and acceptors to expand the library of available DESs. This could lead to the discovery of solvents with even more desirable properties for specific applications. There is also a growing interest in the use of bio-based and renewable components to create more sustainable DESs. Advancements in computational modeling and predictive chemistry may help accelerate the design process for new DESs, allowing researchers to efficiently identify promising candidates for specific applications.

Overall, although these three types of eutectic liquids, including ionic liquids, molten salts, and DESs, are all formed by mixing two or more components, their different compositions result in significant differences in properties such as ionic conductivity. Their corresponding characteristics are summarized in Table 1.

4. Solid Eutectic Materials

4.1. Alloys

Alloys are materials made by combining two or more metallic elements to enhance specific properties such as strength, ductility, corrosion resistance, and thermal conductivity. The study and

application of alloys have played a crucial role in the development of modern technology, engineering, and manufacturing. This exploration of alloys encompasses their history, classification, properties, and applications, highlighting their significance in various industries.

The history of alloys dates back to ancient civilizations when early metalworkers discovered that mixing different metals could yield materials with superior properties compared to pure metals. The use of bronze, an alloy of copper and tin, is one of the earliest examples, marking the beginning of the Bronze Age about 3500 Before Christ (BC). This innovation allowed for the creation of stronger and more durable tools and weapons, significantly impacting societal development. Similarly, the use of iron alloys, particularly steel, emerged around 1200 BC, revolutionizing construction and warfare. Over the centuries, the understanding of alloys has evolved, leading to the development of a wide range of alloy systems tailored for specific applications. Alloys can be broadly classified into two categories: ferrous and nonferrous. Ferrous alloys primarily consist of iron and are used in applications requiring high strength and durability. The most common ferrous alloy is steel, which can be further categorized into carbon steel, alloy steels, and stainless steel based on their composition and properties. Carbon steels are made primarily of iron and carbon, while alloy steels contain additional elements such as manganese, nickel, or chromium to enhance specific characteristics.

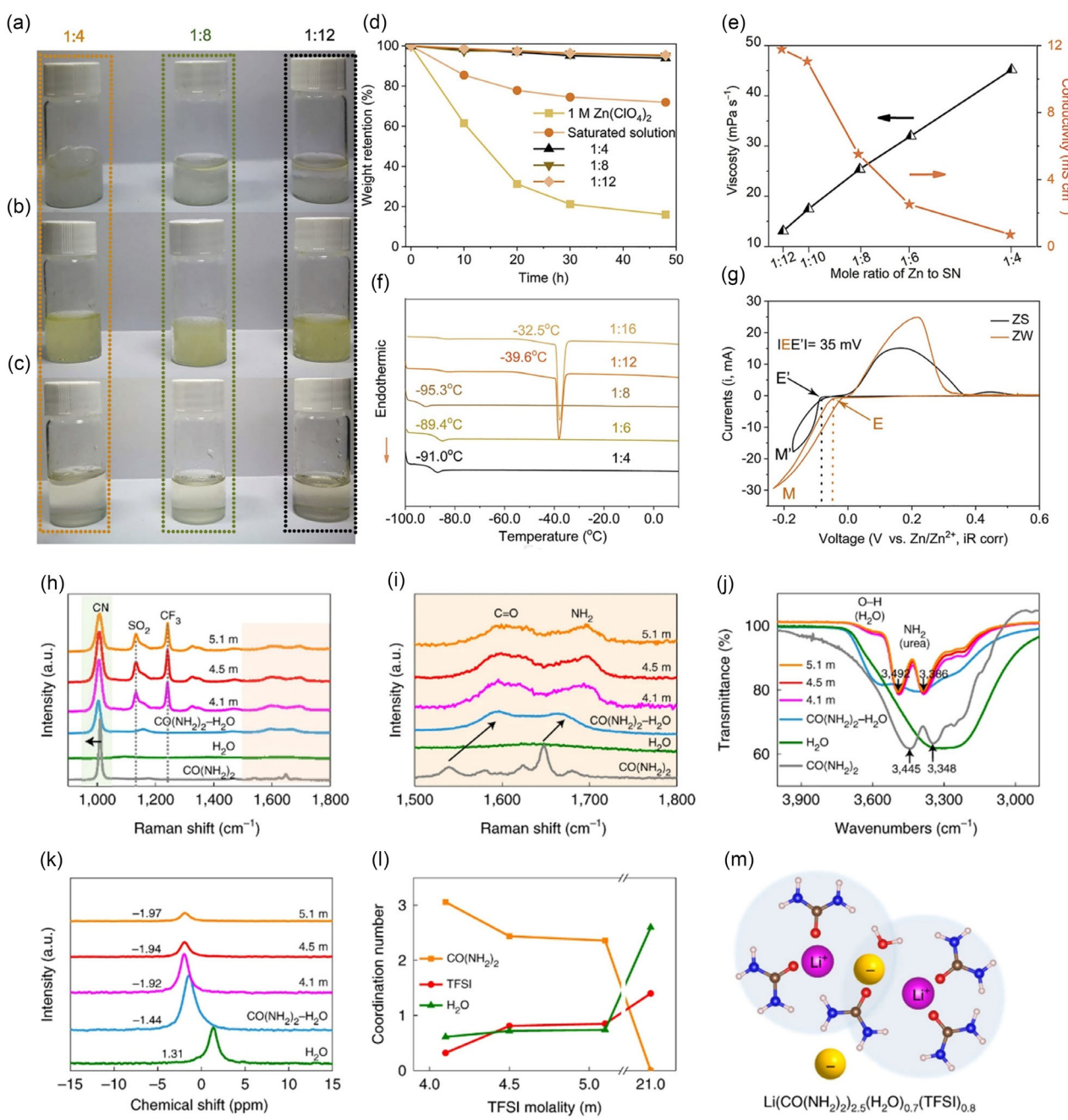


Figure 9. Characterization of the hydrated eutectic electrolytes. a–c) The solubility of (a) $\text{Zn}(\text{SO}_4)_2 \cdot 7\text{H}_2\text{O}$, (b) $\text{Zn}(\text{NO}_3)_2 \cdot 6\text{H}_2\text{O}$, and (c) $\text{Zn}(\text{ClO}_4)_2 \cdot 6\text{H}_2\text{O}$ in SN (the Zn salt/SN molar ratios are 1:4, 1:8, and 1:12 from left to right). d) The weight retention of different electrolytes in the air. e) Viscosity and conductivity of the $\text{Zn}(\text{ClO}_4)_2 \cdot 6\text{H}_2\text{O}/\text{SN}$ eutectic solutions (the molar ratios of $\text{Zn}(\text{ClO}_4)_2 \cdot 6\text{H}_2\text{O}/\text{SN}$ are 1:4, 1:6, 1:8, 1:10, and 1:12). f) DSC data of the $\text{Zn}(\text{ClO}_4)_2 \cdot 6\text{H}_2\text{O}/\text{SN}$ mixtures with the different $\text{Zn}(\text{ClO}_4)_2 \cdot 6\text{H}_2\text{O}/\text{SN}$ molar ratios (1:4, 1:6, 1:8, 1:12, and 1:16). g) Ohmic-corrected CV curves of Zn plating/stripping at scan rate of 1.0 mV s^{-1} . Reproduced with permission from.^[27] Copyright 2020, Springer Nature, Elsevier. h–j) Raman spectra (h,i) and FTIR spectra (j) of the $\text{CO}(\text{NH}_2)_2$, H_2O , $\text{CO}(\text{NH}_2)_2 \cdot \text{H}_2\text{O}$, 4.1, 4.5, and 5.1 m electrolytes. k) The chemical shift of ^{17}O NMR in different electrolytes. l) Coordination numbers of $\text{CO}(\text{NH}_2)_2$, TFSI, and H_2O around Li^+ (within 3.0 Å) for the 4.1, 4.5, and 5.1 m electrolytes compared with 21 m WISE. m) Illustration of the Li^+ primary solvation shell in the 4.5 m electrolyte (H, rose red; Li, purple; C, brown; N, blue; O, red; TFSI, orange). Reproduced with permission from.^[42] Copyright 2022, Springer Nature.

Table 1. Property comparison of ionic liquids, molten salts, and DESs.

	Ionic liquids	Molten salts	DESs
Ionic conductivity	Medium	High	Low-medium
Thermal stability	Medium	High	Low-medium
Cost	High	Medium	Low

Nonferrous alloys, on the other hand, include metals such as aluminum, copper, zinc, and titanium. These alloys are often lighter and more resistant to corrosion compared to ferrous alloys. Aluminum alloys, for instance, are widely used in the aerospace industry due to their high strength-to-weight ratio and excellent corrosion resistance. Copper alloys, including brass and bronze,

are valued for their electrical conductivity and resistance to corrosion, making them ideal for electrical applications and plumbing. The properties of alloys depend on their composition and the processing methods used during their production. The addition of alloying elements can significantly influence the microstructure of the material, leading to enhanced mechanical properties. For example, the introduction of small amounts of carbon into iron can transform its crystalline structure, resulting in the formation of pearlite or martensite, which impart different strength and hardness characteristics. Heat treatment processes such as annealing, quenching, and tempering are also employed to further modify the properties of alloys, allowing for fine-tuning based on specific requirements.

One of the key advantages of alloys is their ability to combine desirable properties from different metals. For instance, steel, an alloy of iron and carbon, exhibits high tensile strength and toughness, making it suitable for construction and manufacturing applications. Stainless steel, which includes chromium, offers excellent corrosion resistance while retaining the strength of steel, making it ideal for use in environments exposed to moisture and chemicals. In addition to their mechanical properties, alloys can also exhibit unique physical and chemical characteristics. For example, adding zinc to copper creates brass, which not only enhances the material's strength but also improves machinability and resistance to tarnishing. Similarly, the combination of aluminum and copper results in a lightweight alloy that maintains good mechanical properties, making it suitable for aerospace applications.

Jiang et al.^[30] reported aluminum–copper alloy layered heterostructures as anode-active materials (Figure 10a–f). These alloys improve the electrochemical reversibility of aluminum ions by using alternating anode α-aluminum and cathode intermetallic Al₂Cu nanolayers in a periodic current coupling, achieving dendrite-free aluminum deposition during stripping/plating cycles. In a symmetric cell configuration with a low oxygen concentration (i.e., 0.13 mg L⁻¹) aqueous electrolyte solution, the flake-like nanostructured eutectic Al₈₂Cu₁₈ alloy electrode enables 2000 h of aluminum stripping/plating with an overpotential of less than ±53 mV. When the Al₈₂Cu₁₈ anode is tested in combination with Al_xMnO₂ cathode materials, the aqueous full cell delivers an energy density of ≈670 Wh kg⁻¹ at 100 mA g⁻¹, and an initial discharge capacity of ≈400 mA h g⁻¹ at 500 mA g⁻¹, with a capacity retention of 83% after 400 cycles. This alloy phase often exhibits unique properties that differ from those of its components, and studying these alloy phases can guide future directions.

Their subsequent study indicated that the eutectic alloying of zinc and aluminum is an effective strategy that utilizes a layered structure composed of alternating zinc and aluminum nanolayers, fundamentally addressing the serious issue of dendrite growth (Figure 10g–j). The layered nanostructure not only facilitates the stripping of zinc from the precursor eutectic Zn₈₈Al₁₂ (at%) alloy but also *in situ* generates a core/shell aluminum/alumina interlayer nanostructure, guiding the subsequent zinc growth. This enables dendrite-free zinc stripping/plating in an oxygen-free aqueous electrolyte for over 2000 h. These excellent

electrochemical performances allow zinc-ion batteries using a Zn₈₈Al₁₂ alloy anode and K_xMnO₂ cathode to provide high-density energy at high power levels, maintaining 100% capacity after 200 h.

Similarly, Yang et al.^[31] designed an interface material composed of a forest-like 3D zinc–copper alloy with engineered surfaces to explore the zinc plating/stripping patterns in dual-cation electrolytes (Figure 11). The 3D nanostructured surface of the zinc–copper alloy was found to effectively regulate the reaction kinetics of the zinc plating/stripping process. The developed interface material suppressed dendrite growth on the anode surfaces of high-performance, durable aqueous zinc-ion batteries in both single- and dual-cation aqueous electrolytes. This work significantly enhances the fundamental understanding of dual-cation intercalation chemistry in aqueous electrochemical systems and provides guidance for exploring high-performance aqueous zinc-ion batteries and other fields.

4.2. Organic Cocrystals

Organic cocrystals are a fascinating class of crystalline materials formed by the association of two or more different organic molecules through noncovalent interactions, such as hydrogen bonding, van der Waals forces, and π–π stacking. These cocrystals exhibit distinct properties that differ from the individual components, offering unique benefits in fields such as pharmaceuticals, materials science, and nanotechnology. The concept of cocrystallization has gained significant attention since the 1990s, as researchers began to recognize the potential of cocrystals to enhance the solubility, stability, and bioavailability of drugs, effectively addressing challenges associated with poorly soluble compounds. The formation of organic cocrystals involves the careful selection of coformers, which can include small organic molecules, polymers, or even biomolecules. The choice of coformers is crucial, as it determines the properties of the resulting cocrystal. For instance, cocrystals can be designed to improve the pharmacokinetic properties of active pharmaceutical ingredients by enhancing their solubility and dissolution rates. This has significant implications for drug formulation, as many drugs suffer from low bioavailability due to poor solubility in aqueous environments. By creating cocrystals with suitable coformers, researchers can increase the effective concentration of the drug in solution, leading to improved therapeutic outcomes.

In addition to their applications in pharmaceuticals, organic cocrystals are also of great interest in materials science. They can exhibit unique optical, electronic, and thermal properties, making them suitable for applications in organic electronics, sensors, and photovoltaic devices.^[32] The ability to engineer cocrystals with specific functional properties allows for the development of advanced materials with tailored characteristics. Moreover, organic cocrystals can also serve as a platform for studying intermolecular interactions, providing insights into the fundamental principles governing crystal formation and stability. The characterization of organic cocrystals is essential to understanding their properties and potential applications.

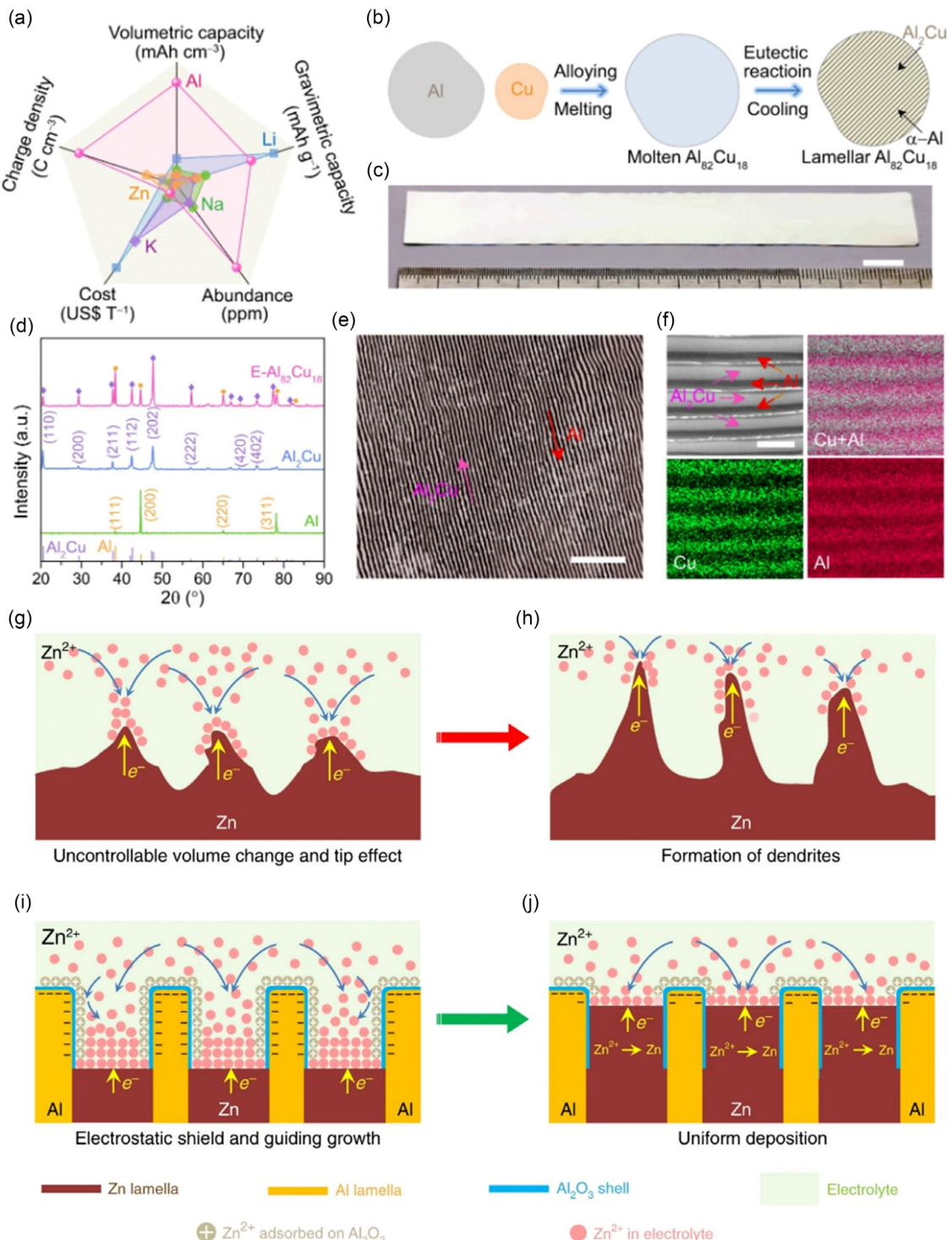


Figure 10. a) Comparisons of electrochemical properties, cost, and abundance for Al, Zn, K, Na, and Li. b) Schematic illustrating the procedure to prepare lamella-nanostructured $\text{E-Al}_{82}\text{Cu}_{18}$ alloy composed of alternating $\alpha\text{-Al}$ (gray) and intermetallic Al_2Cu (dark yellow) lamellas. c) Photograph of as-prepared $\text{E-Al}_{82}\text{Cu}_{18}$ alloy sheets with dimensions of $\approx 13 \text{ cm} \times \approx 1.5 \text{ cm} \times \approx 400 \mu\text{m}$. Scale bar: 1 cm. d) X-ray diffraction (XRD) patterns of $\text{E-Al}_{82}\text{Cu}_{18}$ (pink line), intermetallic Al_2Cu (blue line), and monometallic Al (green line) electrode foils. e) Representative optical micrograph of lamella-nanostructured $\text{E-Al}_{82}\text{Cu}_{18}$ alloy with an interlamellar spacing of $\approx 420 \text{ nm}$. Scale bar: 5 μm . f) SEM backscattered electron image of $\text{E-Al}_{82}\text{Cu}_{18}$ with different contrasts corresponding to $\alpha\text{-Al}$ and intermetallic Al_2Cu lamellas, as well as the corresponding energy-dispersive X-ray spectrometry (EDS) elemental mapping of Cu (in green) and Al (in red). g) Monometallic Zn electrodes with abundant cracks or defects that are produced by uncontrollable volume change in the Zn stripping/plating processes. h) Growth of Zn dendrites triggered by uncontrollable volume change and tip effect. i) Eutectic Zn/Al alloys with a lamellar structure composed of alternative Zn and Al nanolamellas in situ produce core/shell interlayer patterns during the Zn stripping to guide the subsequent Zn plating. j) The Al/ Al_2O_3 interlayer patterns associated with the insulative Al_2O_3 shield facilitate the uniform deposition of Zn.

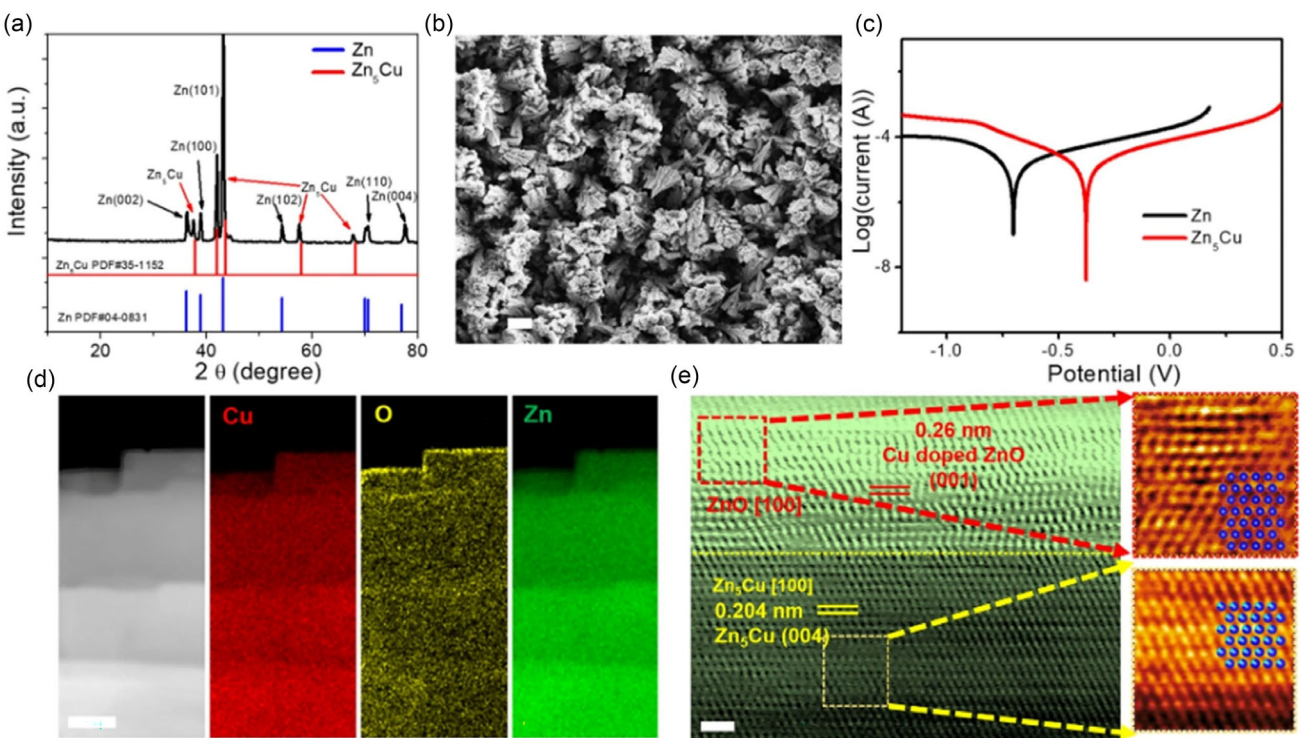


Figure 11. a) XRD pattern of Zn₅Cu. b) SEM image of 3D Zn-Cu anodes. c) Tafel plots of Zn and Zn-Cu anodes. d) EDS mapping of Zn₅Cu. e) Scanning transmission electron microscopy (STEM) image of the ZnO/Zn₅Cu interface.

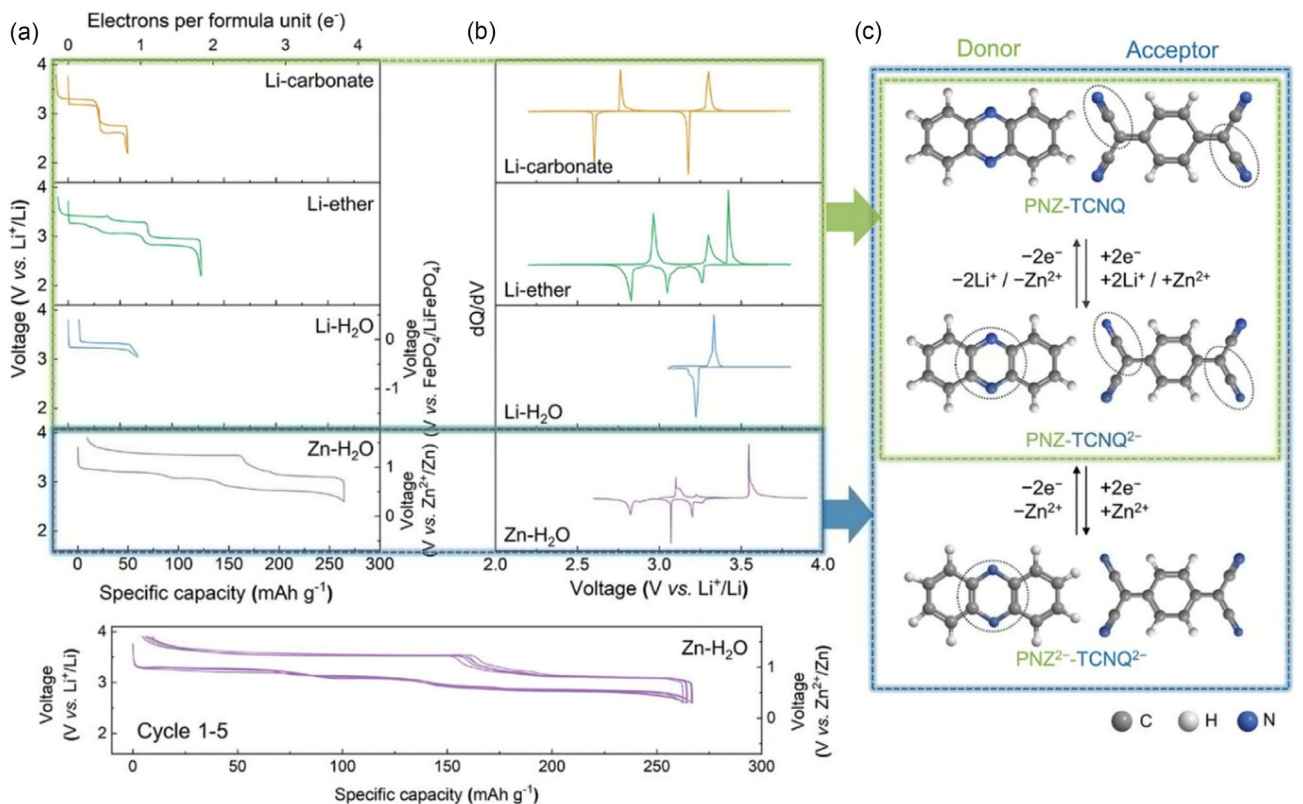


Figure 12. a,b) Capacity–voltage profiles (a) and differential capacity curves (b) of PNZ-TCNQ in lithium ion with carbonates electrolytes, ether electrolytes, aqueous electrolytes, and zinc ion with aqueous electrolytes. c) Suggested redox mechanism of PNZ-TCNQ regarding the four-electron storage. Reproduced with permission from.^[34] Copyright 2025, Wiley-VCH.

Despite their advantages, the development and application of organic cocrystals also face challenges. One significant hurdle is the reproducibility of cocrystal formation, as slight variations in experimental conditions can lead to different crystal forms or the failure to form cocrystals altogether. This variability necessitates a thorough understanding of the factors influencing cocrystal formation, including temperature, solvent choice, and coformer ratios. Furthermore, regulatory considerations in the pharmaceutical industry may pose challenges for the commercialization of cocrystal formulations, requiring extensive testing to ensure safety and efficacy.

Organic charge transfer complexes (OCTCs) composed of redox-active donor and acceptor molecules represent a promising class of electrode materials with the potential to address the low power and poor cycling stability of organic electrodes in rechargeable batteries.^[33] The strong intermolecular interactions in OCTCs, such as $\pi-\pi$ interactions and hydrogen bonding, provide high electronic conductivity and suppress solubility in

solvents. However, despite the inherent redox capabilities of the donor and acceptor molecules, the full redox activity of OCTCs has not been realized. Kang et al.^[34] revealed that the limited redox activity of OCTCs arises from the formation of electrolyte-bound complexes, which weaken the characteristic intermolecular interactions and hinder redox reactions, especially in lithium-based electrolytes (Figure 12a–c). Furthermore, they demonstrated that adjusting the type of electrolyte, particularly using zinc aqueous electrolytes, can significantly alleviate the formation of these complexes and unlock the four-electron redox activity of OCTCs (specifically phenazine (PNZ)-7,7,8,8-tetracyanoquinodimethane (TCNQ), i.e., PNZ-TCNQ), achieving excellent cycling stability with 88% of the maximum capacity retained after 100 cycles. Remarkably, the complete redox reactions enabled unprecedented high electrode-level energy densities, providing $\approx 10 \text{ mA h cm}^{-2}$ of areal capacity in zinc aqueous batteries (with electrodes 580 μm thick). These findings elucidate the complex interactions between organic electrodes and

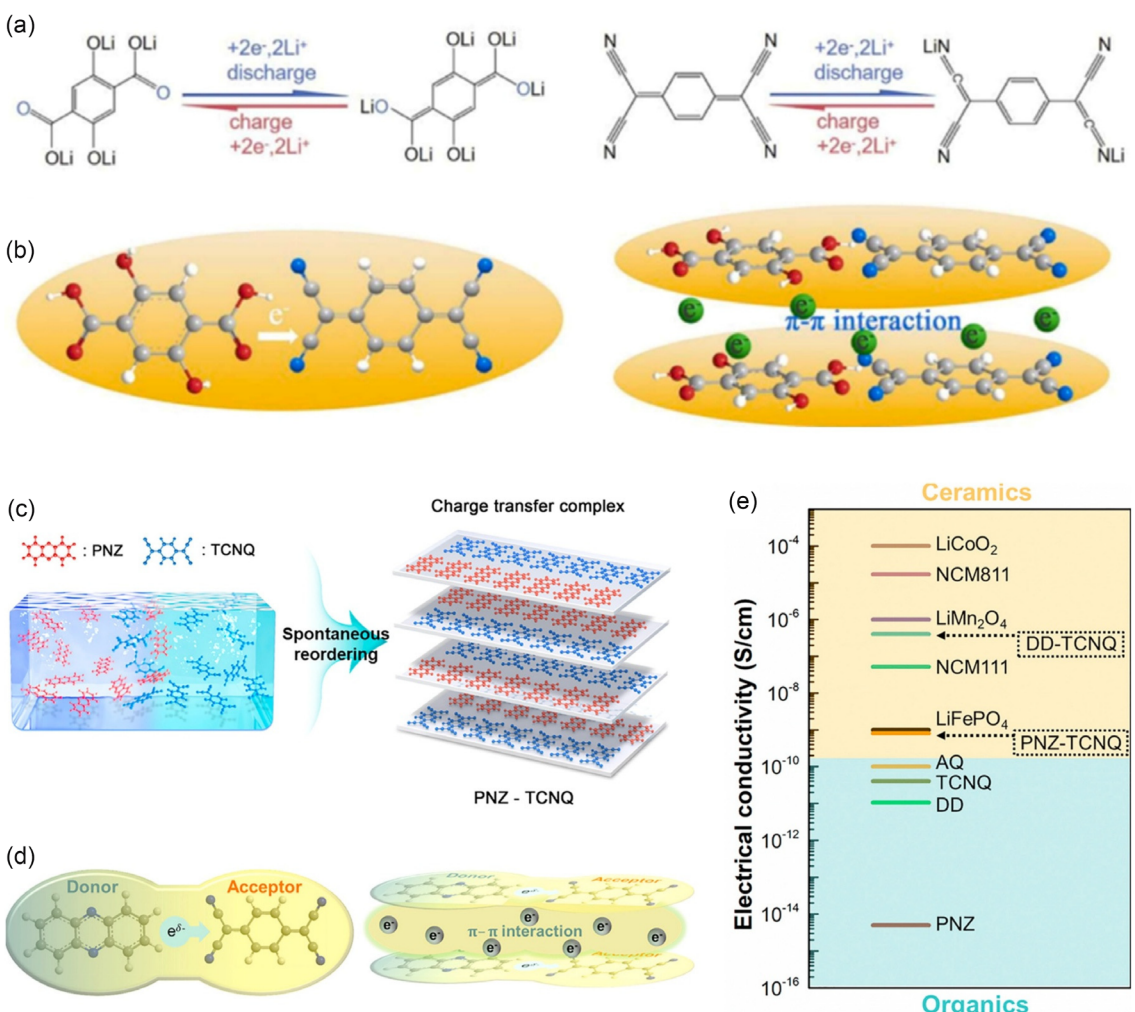


Figure 13. a) Reaction formula for $\text{Li}_4\text{C}_8\text{H}_2\text{O}_6$ and TCNQ. b) Schematic representation of $\text{Li}_4\text{C}_8\text{H}_2\text{O}_6$ and TCNQ interactions. Reproduced with permission from.^[35] Copyright 2023, Elsevier. c) Concepts of OCTC. d) Conceptual diagram and brief structural description of the OCTC PNZ-TCNQ. e) Electrical conductivities of representative inorganic and organic redox active species and OCTCs. Reproduced with permission from.^[36] Copyright 2019, Elsevier.

electrolytes in charge storage mechanisms, highlighting the importance of electrolyte design in the development of organic electrode materials.

Wu et al.^[35] developed a charge transfer complex for all-solid-state batteries by combining 2,5-dihydroxyterephthalic acid ($\text{Li}_4\text{C}_8\text{H}_2\text{O}_6$) and tetracyanoquinodimethane (TCNQ) in a 1,3-dioxolane (DOL) solvent at room temperature (Figure 13a, b). The $\text{Li}_4\text{C}_8\text{H}_2\text{O}_6$ -TCNQ complex acts as an electron donor/acceptor, forming enhanced electron clouds through π - π interactions that facilitate electron transport. The electronic conductivity of the charge transfer complex $\text{Li}_4\text{C}_8\text{H}_2\text{O}_6$ -TCNQ increased to 7×10^{-5} S/cm, which is three orders of magnitude higher than that of the two original materials and significantly exceeds that of most traditional organic cathodes. The $\text{Li}_4\text{C}_8\text{H}_2\text{O}_6$ -TCNQ electrode exhibited a discharge capacity of 172 mA g⁻¹ at 0.5 C, ≈ 2.5 times that of $\text{Li}_4\text{C}_8\text{H}_2\text{O}_6$, and maintained stable cycling for 100 cycles at 2 C. These results demonstrate that enhancing the electron cloud through π - π interactions in charge transfer complexes is an effective pathway for the practical application of organic cathodes in sulfide-based all-solid-state batteries.

Jiang et al.^[36] reported on OCTCs, a novel class of electrode materials that possess inherent high conductivity and low solubility, potentially overcoming the long-standing deficiencies of organic electrodes (Figure 13c–e). By forming charge transfer complexes of phenazine-7,7,8,8-tetracyanoquinodimethane and dibenzo-1,4-dioxin-7,7,8,8-tetracyanoquinodimethane through a room-temperature process, they can enhance conductivity and reduce solubility, achieving high power and cycling performance that far exceeds that of each individual component. This finding demonstrates the universal applicability of charge transfer complexes, which can simultaneously improve conductivity and mitigate the shortcomings of existing single-component organic electrode materials. Furthermore, it opens up an unexplored pathway for developing high-performance organic electrode materials by exploring various combinations of donor-acceptor monomers with different stoichiometries.

In conclusion, organic cocrystals represent a promising area of research with the potential to revolutionize various fields, particularly in pharmaceuticals and materials science.^[37] Their ability to enhance solubility and stability while offering unique properties makes them valuable for developing advanced materials and drug formulations. Ongoing research continues to explore new coforming strategies, characterization techniques, and applications, paving the way for innovative solutions to modern challenges in drug delivery and material design. As our understanding of organic cocrystals deepens, their role in advancing technology and improving health outcomes is expected to grow significantly.

5. Summary and Outlook

Eutectic materials offer an exciting pathway for next-generation energy storage and conversion devices. Their distinctive phase diagrams and melting point depressions enable both excellent ionic and electronic transport. By precisely adjusting component ratios, researchers can optimize electrochemical performance

and improve energy density and efficiency in batteries, supercapacitors, and fuel cells.

Despite these advances, several critical challenges remain. First, the rational design of eutectic compositions is still in its infancy. Integrating artificial intelligence (AI)-driven prediction with high-throughput synthesis and screening will be essential to establish clear design rules and practical formulation pathways. Second, a deeper understanding of how eutectics form and function at the atomic scale requires advanced characterization (e.g., *in situ* electron microscopy and synchrotron X-ray scattering) and complementary theoretical modeling. Third, many unique properties of eutectic systems (e.g., tunable solvation structures and reversible phase transitions under electrochemical cycling) have yet to be fully explored or exploited. Fourth, scalable, reproducible synthesis methods must be developed and standardized to translate lab-scale discoveries into real-world devices.

Looking ahead, the integration of predictive computation, *in situ* characterization, and tailored synthesis is expected to accelerate the discovery of high-performance eutectic electrolytes, electrodes, and hybrid systems. Eutectic materials hold significant promise for postlithium energy storage, particularly in Mg-, Al-, Zn-based batteries, where their tunable solvation structures and low melting points can enable reversible metal ions plating/stripping and suppress side reactions. Moreover, the inherent fluidity of eutectics may help mitigate dendrite formation by promoting uniform ion flux at the electrode–electrolyte interface. These attributes open new pathways toward safe, high-capacity multivalent batteries. We hope this review will provide a useful roadmap for researchers seeking to exploit the unique phase behavior of eutectics and translate it into tangible improvements in energy density, power output, and long-term stability.

Conflict of Interest

The authors declare no conflict of interest.

Keywords: alloy materials · deep eutectic solvents · ionic liquids · molten salts · organic cocrystals

- [1] a) R. V. Noorden, *Nature* **2014**, *507*, 26; b) J. Janek, W. G. Zeier, *Nat. Energy* **2016**, *1*, 4; c) D. Larcher, J. M. Tarascon, *Nat. Chem.* **2015**, *7*, 19.
- [2] a) G. Liang, X. Li, Y. Wang, S. Yang, Z. Huang, Q. Yang, D. Wang, B. Dong, M. Zhu, C. Zhi, *Nano Res. Energy* **2022**, *1*, e9120002; b) Y. Tian, S. Chen, Y. He, Q. Chen, L. Zhang, J. Zhang, *Nano Res. Energy* **2022**, *1*, e9120025.
- [3] a) L. Geng, X. Wang, K. Han, P. Hu, L. Zhou, Y. Zhao, W. Luo, L. Mai, *ACS Energy Lett.* **2021**, *7*, 247; b) P. Jiang, L. Chen, H. Shao, S. Huang, Q. Wang, Y. Su, X. Yan, X. Liang, J. Zhang, J. Feng, Z. Liu, *ACS Energy Lett.* **2019**, *4*, 1419; c) J. Kim, B. Koo, J. Lim, J. Jeon, C. Lim, H. Lee, K. Kwak, M. Cho, *ACS Energy Lett.* **2021**, *7*, 189.
- [4] H. Hong, J. Zhu, Y. Wang, Z. Wei, X. Guo, S. Yang, R. Zhang, H. Cui, Q. Li, D. Zhang, C. Zhi, *Adv. Mater.* **2024**, *36*, e2308210.
- [5] a) X. Lin, G. Zhou, M. J. Robson, J. Yu, S. C. T. Kwok, F. Ciucci, *Adv. Funct. Mater.* **2021**, *32*, 2109322; b) J. Wu, Q. Liang, X. Yu, Q. F. Lu, L. Ma, X. Qin, G. Chen, B. Li, *Adv. Funct. Mater.* **2021**, *31*, 2011102; c) P. Jaumaux, Q. Liu, D. Zhou, X. Xu, T. Wang, Y. Wang, F. Kang, B. Li, G. Wang, *Angew. Chem. Int. Ed.* **2020**, *59*, 9134.

- [6] a) X. Pei, Y. Li, T. Ou, X. Liang, Y. Yang, E. Jia, Y. Tan, S. Guo, *Angew. Chem. Int. Ed.* **2022**, e202205075; b) H. Qiu, R. Hu, X. Du, Z. Chen, J. Zhao, G. Lu, M. Jiang, Q. Kong, Y. Yan, J. Du, X. Zhou, G. Cui, *Angew. Chem. Int. Ed.* **2022**, *61*, e202113086; c) A. P. Abbott, J. C. Barron, K. S. Ryder, D. Wilson, *Chemistry* **2007**, *13*, 6495.
- [7] a) B. B. Hansen, S. Spittle, B. Chen, D. Poe, Y. Zhang, J. M. Klein, A. Horton, L. Adhikari, T. Zelovich, B. W. Doherty, B. Gurkan, E. J. Maginn, A. Ragauskas, M. Dadmun, T. A. Zawodzinski, G. A. Baker, M. E. Tuckerman, R. F. Savinell, J. R. Sangoro, *Chem. Rev.* **2021**, *121*, 1232; b) E. L. Smith, A. P. Abbott, K. S. Ryder, *Chem. Rev.* **2014**, *114*, 11060.
- [8] D. Yu, Z. Xue, T. Mu, *Chem. Soc. Rev.* **2021**, *50*, 8596.
- [9] Z. Tian, Y. Zou, G. Liu, Y. Wang, J. Yin, J. Ming, H. N. Alshareef, *Adv. Sci.* **2022**, *9*, e2201207.
- [10] A. M. Navarro-Suárez, P. Johansson, *J. Electrochem. Soc.* **2020**, *167*, 070511.
- [11] H. Cruz, N. Jordão, L. C. Branco, *Green Chem.* **2017**, *19*, 1653.
- [12] H. Hong, Y. Wang, Y. Zhang, B. Han, Q. Li, X. Guo, Y. Guo, A. Chen, Z. Wei, Z. Huang, Y. Zhao, J. Fan, C. Zhi, *Adv. Mater.* **2024**, *36*, e2407150.
- [13] H. Yang, H. Li, J. Li, Z. Sun, K. He, H. M. Cheng, F. Li, *Angew. Chem. Int. Ed.* **2019**, *58*, 11978.
- [14] a) D. L. Ye, B. Luo, G. M. Lu, L. Z. Wang, *Sci. Bull.* **2015**, *60*, 1042; b) S. K. Das, S. Mahapatra, H. Lahan, *J. Mater. Chem. A* **2017**, *5*, 6347; c) M. Wang, F. Zhang, C. S. Lee, Y. B. Tang, *Adv. Energy Mater.* **2017**, *7*, 1700536.
- [15] M. C. Lin, M. Gong, B. Lu, Y. Wu, D. Y. Wang, M. Guan, M. Angell, C. Chen, J. Yang, B. J. Hwang, H. Dai, *Nature* **2015**, *520*, 325.
- [16] a) P. Ruan, S. Liang, B. Lu, H. J. Fan, J. Zhou, *Angew. Chem. Int. Ed.* **2022**, *61*, 202200598; b) M. Song, H. Tan, D. Chao, H. J. Fan, *Adv. Funct. Mater.* **2018**, *28*, 1802564; c) G. Z. Fang, J. Zhou, A. Q. Pan, S. Q. Liang, *ACS Energy Lett.* **2018**, *3*, 2480.
- [17] Q. D. Truong, M. Kempaiah Devaraju, D. N. Nguyen, Y. Gambe, K. Nayuki, Y. Sasaki, P. D. Tran, I. Honma, *Nano Lett.* **2016**, *16*, 5829.
- [18] M. Zhao, J. Rong, F. Huo, Y. Lv, B. Yue, Y. Xiao, Y. Chen, G. Hou, J. Qiu, S. Chen, *Adv. Mater.* **2022**, *34*, e2203153.
- [19] L. Yu, J. Huang, S. Wang, L. Qi, S. Wang, C. Chen, *Adv. Mater.* **2023**, *35*, e2210789.
- [20] Q. Pang, J. Meng, S. Gupta, X. Hong, C. Y. Kwok, J. Zhao, Y. Jin, L. Xu, O. Karahan, Z. Wang, S. Toll, L. Mai, L. F. Nazar, M. Balasubramanian, B. Narayanan, D. R. Sadoway, *Nature* **2022**, *608*, 704.
- [21] J. Meng, X. Hong, Z. Xiao, L. Xu, L. Zhu, Y. Jia, F. Liu, L. Mai, Q. Pang, *Nat. Commun.* **2024**, *15*, 596.
- [22] M. Yoon, Y. Dong, Y. Huang, B. Wang, J. Kim, J.-S. Park, J. Hwang, J. Park, S. J. Kang, J. Cho, J. Li, *Nat. Energy* **2023**, *8*, 482.
- [23] Q. Zhang, K. De Oliveira Vigier, S. Royer, F. Jerome, *Chem. Soc. Rev.* **2012**, *41*, 7108.
- [24] B. Gurkan, H. Squire, E. Pentzer, *J. Phys. Chem. Lett.* **2019**, *10*, 7956.
- [25] X. Ge, C. Gu, X. Wang, J. Tu, *J. Mater. Chem. A* **2017**, *5*, 8209.
- [26] M. K. Tran, M.-T. F. Rodrigues, K. Kato, G. Babu, P. M. Ajayan, *Nat. Energy* **2019**, *4*, 339.
- [27] W. H. Yang, X. F. Du, J. W. Zhao, Z. Chen, J. J. Li, J. Xie, Y. J. Zhang, Z. L. Cui, Q. Y. Kong, Z. M. Zhao, C. G. Wang, Q. C. Zhang, G. L. Cui, *Joule* **2020**, *4*, 1557.
- [28] J. Xu, X. Ji, J. Zhang, C. Yang, P. Wang, S. Liu, K. Ludwig, F. Chen, P. Kofinas, C. Wang, *Nat. Energy* **2022**, *7*, 186.
- [29] D. De Sloovere, D. E. P. Vanpoucke, A. Paulus, B. Joos, L. Calvi, T. Vranken, G. Reekmans, P. Adriaensens, N. Eshraghi, A. Mahmoud, F. Boschini, M. Safari, M. K. Van Bael, A. Hardy, *Adv. Energy Sustainability Res.* **2022**, *3*, 2100159.
- [30] Q. Ran, H. Shi, H. Meng, S. P. Zeng, W. B. Wan, W. Zhang, Z. Wen, X. Y. Lang, Q. Jiang, *Nat. Commun.* **2022**, *13*, 576.
- [31] H. Tian, G. Feng, Q. Wang, Z. Li, W. Zhang, M. Lucero, Z. Feng, Z. L. Wang, Y. Zhang, C. Zhen, M. Gu, X. Shan, Y. Yang, *Nat. Commun.* **2022**, *13*, 7922.
- [32] a) M. Lee, J. Hong, J. Lopez, Y. Sun, D. Feng, K. Lim, W. C. Chueh, M. F. Toney, Y. Cui, Z. Bao, *Nat. Energy* **2017**, *2*, 861; b) L. Jiang, Y. Lu, C. Zhao, L. Liu, J. Zhang, Q. Zhang, X. Shen, J. Zhao, X. Yu, H. Li, X. Huang, L. Chen, Y.-S. Hu, *Nat. Energy* **2019**, *4*, 495; c) D. Feng, T. Lei, M. R. Lukatskaya, J. Park, Z. Huang, M. Lee, L. Shaw, S. Chen, A. A. Yakovenko, A. Kulkarni, J. Xiao, K. Fredrickson, J. B. Tok, X. Zou, Y. Cui, Z. Bao, *Nat. Energy* **2018**, *3*, 30.
- [33] a) L. Zhao, A. E. Lakraychi, Z. Chen, Y. Liang, Y. Yao, *ACS Energy Lett.* **2021**, *6*, 3287; b) W. Wang, V. S. Kale, Z. Cao, S. Kandambeth, W. Zhang, J. Ming, P. T. Parvatkar, E. Abou-Hamad, O. Shekhah, L. Cavallo, M. Eddaoudi, H. N. Alshareef, *ACS Energy Lett.* **2020**, *5*, 2256; c) T. Chen, H. Banda, J. Wang, J. J. Oppenheim, A. Franceschi, M. Dincă, *ACS Cent. Sci.* **2024**, *10*, 569.
- [34] S. Lee, J. Kim, J. Hong, K. Kang, *Adv. Energy Mater.* **2024**, *15*, 2404116.
- [35] F. Song, Z. Wang, T. Ma, L. Chen, H. Li, F. Wu, *Nano Energy* **2023**, *117*, 108893.
- [36] S. Lee, J. Hong, S.-K. Jung, K. Ku, G. Kwon, W. M. Seong, H. Kim, G. Yoon, I. Kang, K. Hong, H. W. Jang, K. Kang, *Energy Stor. Mater.* **2019**, *20*, 462.
- [37] a) M. Yu, N. Chandrasekhar, R. K. M. Raghupathy, K. H. Ly, H. Zhang, E. Dmitrieva, C. Liang, X. Lu, T. D. Kuhne, H. Mirhosseini, I. M. Weidinger, X. Feng, *J. Am. Chem. Soc.* **2020**, *142*, 19570; b) S. Wang, Q. Wang, P. Shao, Y. Han, X. Gao, L. Ma, S. Yuan, X. Ma, J. Zhou, X. Feng, B. Wang, *J. Am. Chem. Soc.* **2017**, *139*, 4258; c) K. W. Nam, H. Kim, Y. Beldjoudi, T. W. Kwon, D. J. Kim, J. F. Stoddart, *J. Am. Chem. Soc.* **2020**, *142*, 2541; d) M. L. Aubrey, J. R. Long, *J. Am. Chem. Soc.* **2015**, *137*, 13594; e) G. Dawut, Y. Lu, L. Miao, J. Chen, *Inorg. Chem. Front.* **2018**, *5*, 1391; f) V. Nemec, N. Škvorc, D. Cinčić, *CrystEngComm* **2015**, *17*, 6274.

Manuscript received: June 3, 2025

Revised manuscript received: July 9, 2025

Version of record online: